Bioorganic Chemistry xxx (xxxx) xxx

Contents lists available at ScienceDirect

Bioorganic Chemistry

journal homepage: www.elsevier.com/locate/bioorg

5-HT_{1A} targeting PARCEST agent DO3AM-MPP with potential for receptor imaging: Synthesis, physico-chemical and MR studies

Anju [a,b], Shubhra Chaturvedi [b,*], Vishakha Chaudhary [a,b], Pradeep Pant [c], Preeti Jha [d], Senthil S. Kumaran [e], Firasat Hussain [a], Anil Kumar Mishra [b,*]

[a] Department of Chemistry, University of Delhi, North Campus, Delhi 110007, India
[b] Division of Cyclotron and Radiopharmaceutical Sciences, Institute of Nuclear Medicine and Allied Sciences, Defence Research and Development Organization, Brig. S. K Mazumdar Road, Timarpur, Delhi 110054, India
[c] Department of Chemistry, Indian Institute of Technology, Hauz Khas, New Delhi 110016, India
[d] Department of Immunology, Genetics and Pathology, Uppsala University, 75185 Uppsala, Sweden
[e] All India Institute of Medical Sciences, Ansari Nagar, New Delhi 110029, India

ARTICLE INFO

Keywords:
Chemical Exchange Saturation Transfer
Computational Studies
Density Functional Theory
Water Residence Lifetime
Longitudinal and Transverse relaxivity
Fluorescence quenching

ABSTRACT

Contrast enhancement in MRI using magnetization or saturation transfer techniques promises better sensitivity, and faster acquisition compared to T_1 or T_2 contrast. This work reports the synthesis and evaluation of 5-HT_{1A} targeted PARACEST MRI contrast agent using 1,4,7,10-tetraazacycloDOdecane-4,7,10-triacetAMide (DO3AM) as the bifunctional chelator, and 5-HT_{1A}-antagonist methoxyphenyl piperazine (MPP) as a targeting unit. The multi-step synthesis led to the MPP conjugated DO3AM with 60% yield. CEST-related physicochemical parameters were evaluated after loading DO3AM-MPP with paramagnetic MRI active lanthanides: Gadolinium (Gd-DO3AM-MPP) and Europium (Eu-DO3AM-MPP). Luminescence lifetime measurements with Eu-DO3AM-MPP and computational DFT studies using Gd-DO3AM-MPP revealed the coordination of one water molecule (q = 1.43) with metal-water distance (r_M-H_2O) of 2.7 Å and water residence time (τ_m) of 0.23 ms. The dissociation constant of K_d 62 ± 0.02 pM as evaluated from fluorescence quenching of 5-HT_{1A} (protein) and docking score of −4.81 in theoretical evaluation reflect the binding potential of the complex Gd-DO3AM-MPP with the receptor 5-HT_{1A}. Insights of the docked pose reflect the importance of NH_2 (amide) and aromatic ring in Gd-DO3AM-MPP while interacting with Ser 374 and Phe 370 in the antagonist binding pocket of 5-HT_{1A}. Gd-DO3AM-MPP shows longitudinal relaxivity 5.85 $mM^{-1}s^{-1}$ with a water residence lifetime of 0.93 ms in hippocampal homogenate containing 5-HT_{1A}. The potentiometric titration of DO3AM-MPP showed strong selectivity for Gd^{3+} over physiological metal ions such as Zn^{2+} and Cu^{2+}. The *in vitro* and *in vivo* studies confirmed the minimal cytotoxicity and presential binding of Gd-DO3AM-MPP with 5-HT_{1A} receptor in the hippocampus region of the mice. Summarizing, the complex Gd-DO3AM-MPP can have a potential for CEST imaging of 5-HT_{1A} receptors.

1. Introduction

Magnetic Resonance Imaging (MRI) is among the most sought-after molecular imaging techniques mainly due to low invasiveness, excellent soft-tissue contrast, no ionizing radiation, and good temporal-spatial resolution. [1] The variation in the concentration and the bound state of water molecules in different tissues results in contrast in MRI. Further, image contrast in MRI can be altered either by variation in pulse sequences or by introducing certain chemical entities. The chemical entities, popularly referred to as contrast reagents in the jargon of imaging sciences, have been widely applied and researched extensively. Mechanistically, the contrast agents alter the relaxation rate of water protons in their vicinity resulting in contrast. [2] Both longitudinal (T_1) or (and) transverse (T_2) relaxations can be affected by contrast agents. For instance, lanthanide-based contrast agents affect mainly T_1, whereas superoxide or the iron nanoparticles alter T_2. [3,4] The lanthanide-

Abbreviations: 5-HT_{1A}, 5-hydroxy tryptamine Receptor (Class-1A); MRI, Magnetic Resonance Imaging; CEST, Chemical Exchange Saturation Transfer; MPP, Methoxyphenyl piperazine; Gd-DO3AM, Gadolinium 2, 2′, 2′'-(1,4,7,10 -tetraazacyclododecane-1, 4, 7triyl) triacetamide; 2D, Two Dimensional; 3D, Three Dimensional.

* Corresponding authors.
E-mail addresses: shubhra@inmas.drdo.in (S. Chaturvedi), akmishra@inmas.drdo.in (A. Kumar Mishra).

https://doi.org/10.1016/j.bioorg.2020.104487
Received 4 November 2020; Accepted 17 November 2020
Available online 24 November 2020

based contrast agents, particularly gadolinium complexes, hold a considerable share in MRI and account for 30% of MRI scans. The complexes are tuned to study fluctuations in the cellular micro-environment by being responsive or are targeted -gadolinium complexes as T_1 agents have spawned interest in receptor imaging. [5,6] However, the sensitivity required to detect the low concentration and perturbation in receptor expression has remained a challenge for an effective MRI contrast agent, even though few examples have been reported for ex-vivo targeting of neuro-receptors (Fig. 1 [7–10].

Parametric analysis for MRI based receptor imaging reveals the importance of increasing the relaxation rate while designing sensitive gadolinium complexes. Relaxation rate or relaxivity is a complex parameter relying on the variables: (i) rotational correlation time (τ_R 0.2–0.5 ns) (ii) rate of water exchange ($\tau_M < 100$ ns) and, (iii) contribution from water molecules in the second sphere of hydration. [9] While tuning the three variables, the physical and stability constraints limit the increase in relaxivity much lower than the theoretically possible values and restrict the sensitivity of the gadolinium complexes.

The mechanistically alternate method that is chemical exchange saturation transfer, to achieve contrast, relies on magnetization transfer instead of relaxivity. The contrast produced is a darker image instead of brighter contrast as provided by T_1 modulating contrast agents. CEST contrast agents have around two order higher sensitivity, fast acquisition, and better spatial resolution. [11,12,1]

In order to further explore the utility of CEST contrast agents, we have attempted to design a CEST agent with Gadolinium and Europium and evaluate for serotonin receptors imaging. Targeting towards 5-HT_{1A} receptors was accomplished by well-exploited antagonist pharmacophore, methoxyphenyl piperazine (MPP). MPP as targeting moiety has been reported for a gamut of PET/ SPECT imaging (nuclear imaging) and MRI-T_1 contrast agents. [13,14] The complex was studied for physical parameters that affect CEST viz., coordinating water molecules and water exchange through luminescence lifetime measurements and theoretical calculations, alteration in T_1 and relaxivity through MRI and targeting ability through evaluation of binding parameters using fluorescence quenching and theoretical predictions.

2. Materials and methods

1-(2-methoxyphenylpiprazine), 1,4,7,10-tetraazacyclododecane (cyclen), 1-bromo-3-chloropropane, potassium carbonate, sodium bicarbonate, trifluoroacetic acid, di-*tert*-butyl-dicarbonate and sodium sulphate were purchased from Sigma-Aldrich. Metal salts ($GdCl_3{\cdot}6H_2O$, $EuCl_3{\cdot}6H_2O$) were purchased from Aldrich with 99.9% purity. Acetonitrile (HPLC Grade), Dichloromethane (HPLC Grade), Chloroform (HPLC Grade) were obtained from Merck Ltd., India, and used as such without any purification. Compounds Purifications carried out using column chromatography using silica gel having mesh size (60–120 μm). TLC was run on silica gel coated aluminum sheets (silica gel 60, F254, Merck) and analyzed under UV detection set at fixed wavelength 254 nm. ^1H and ^{13}C on the Jeol Model JNM-EXCP 400 MHz system at Delhi University. Chemical Shift (□) represented in ppm with respect to TMS. High-Resolution mass spectroscopy (ESI-MS) was performed on Agilent G6530AA (LC-HRMS-Q-TOF) at Delhi University. Ultra-Pure Liquid Chromatography (ESI-MS) was performed at Jubilant Pvt. Ltd., Noida, India. In vitro and in vivo MR studies were performed using 7 T Bio-Spec USR 70/20 animal MRI Scanner at All India Institute of Medical Sciences, Delhi India. Computational studies were performed using SchrÖdinger Software LLC, New York, 2017 Maestro.

2.1. Synthesis and characterization

2.1.1. 1-(3-Chloropropyl)-4-(2-methoxy-phenyl)-piperazine (1)

A solution of 1, 3-bromochloropropane (1.22 g, 7.80 mmol) dissolved in acetonitrile was added to a stirring solution of 1-(2-Methoxyphenyl)-piperazine (1 g, 5.20 mmol) and potassium carbonate (2.1 g, 15.60 mmol) in 20 ml acetonitrile at 70 °C. The mixture was refluxed for 24 h. The progress of reaction was monitored by TLC (DCM:MeOH 9:1). After the completion of reaction, inorganic salts were separated by filtrations and solution of reaction mixture was evaporated to dryness under vacuum to get yellow-green liquid oil. The compound was purified by column chromatography using (60–120) mesh size silica, the desired product was eluted at 1% MeOH in DCM ($R_f = 0.75$) yield (75%) which was evaporated to get light blue liquid oil.

^1H NMR (400MHz,$CDCl_3$) (δ in ppm) $\delta = 6.91–6.89$ (m, 4H, ArH, $J =$ 2 Hz) (aromatic region), $\delta = 3.83$ (s, 3H, OCH_3), $\delta = 3.11$ (piperazine ring hydrogens) (br, s, 4H, $–CH_2$), $\delta = 2.69$ (br, s, 4H, $–CH_2$) (piperazine ring hydrogens), $\delta = 2.49$ (t, $J = 10.8$ Hz, 2H) $\delta = 1.84$ (quintet, $J = 10.8$ Hz, 2H), $\delta = 1.22$ (t, $J = 10.8$ Hz, 2H), ^{13}C NMR (100 MHz $CDCl_3$) 25 °C, 152.1, 141.0, 122.9, 120.9, 111.0 (aromatic carbons), 56.0, 55.2, 53.3, 50.3, 30.8, 23.7; MS(ESI^+) *m/z* calculated for $C_{14}H_{21}ClN_2O$ is 268.1342 found $(M + H)^+$ 269.1407.

2.1.2. 1, 4, 7, 10 tetraaza-Cyclododecane-1,4,7-tricarboxylic acid tri-tert-butyl ester (2)

To a solution of cyclen (1 g, 2.314 mmol) and triethylamine (710 mg, 7.021 mmol) in chloroform, solution of di-*tert*- butyl dicarbonate (3.396 g, 17.414 mmol) in chloroform was added dropwise over a course of 2 h at 0 °C. Then resulting solution was allowed to warm to room temperature and stir for additional 18 h. The reaction mixture was filtered, and solvents were removed under vacuum. The dried mixture was then washed with water (2 × 100 ml) and the organic layer was dried over Na_2SO_4, and the solvents were removed under vacuum. Further the residue was purified by column chromatography over a silica gel using mesh size (60–120) $R_f = 0.5$ (50% EtOAc: PET Ether) and the product was eluted at 60% P-ET Ether in ethylacetate with yield 70%. ^1H NMR (400 MHz, $CDCl_3$) (in ppm) ^1H NMR (400 MHz, $CDCl_3$) $\delta = 3.57$, (s, 4H, br), □=3.35 (s, 8H), $\delta = 2.80$ (s, 4H, br), $\delta = 1.42$ (doublet, $J = 9.6$ Hz, 27H). ^{13}C NMR C═O $\delta = 151.9$, ($C(CH_3)_3$), $\delta = 81.2$, $\delta = 51.0$ (ring CH_2), $\delta = 49.5$ (ring CH_2), $\delta = 28.7$, (ring CH_2), $\delta = 27.5$ ($C(CH_3)_3$. MS (ESI +) *m/z* calculated for $C_{33}H_{44}N_4O_6$ is 472.3263 found $(M + H)^+$ 473.3335.

2.1.3. 10-(3-(4-(2-Methoxy-phenyl)-piperazin-1-yl)-propyl)-1, 4, 7, 10 teraaza-cyclododecane-1,4,7tricarboxylic acid tri-tert-butyl ester (3)

To a solution of 2 (500 mg, 1.05 mmol) and K_2CO_3 (438.94 mg, 3.177 mmol) in acetonitrile, 1 was dissolved in acetonitrile (1.05 mmol,

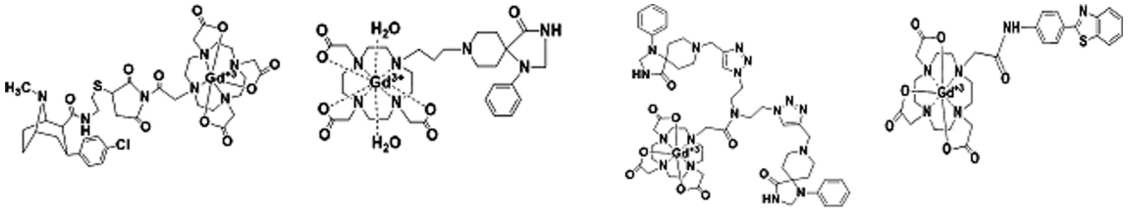

Fig. 1. Gadolinium based T_1 contrast agents for receptor imaging.

283.89 mg) was added dropwise and this mixture was allowed to stir for 48 h at 70 °C. The progress of reaction of mixture was monitored by running TLC (40% PET Ether in ethyl-acetate). Further inorganic salts were filtered, and solution of reaction mixture was evaporated to dryness under dryness to get brownish liquid oil. The compound was purified by column chromatography using (60–120) mesh and the desired product was eluted at 50% PET Ether in ethylacetate with yield 45% (R_f = 0.32). ^{1}H NMR (400 MHz, $CDCl_3$) (δ in ppm) δ = 7.007–6.835 Aromatic-H (4H, m J = 2 Hz), δ = 4.12 (2H, triplet, J = 7.6 Hz CH_2) linker, δ = 3.84 (OCH_3, 3H, s), δ = 3.60 (cyclen ring CH_2 4H, s), δ = 3.26 (cyclen ring CH_2, 8H, s) δ = 3.08 (CH_2 Piperazine ring, 4H, s br), δ = 2.82 (ring CH_2, 4H, s), δ = 2.65 (4H, s br) piperazine ring, δ = 2.48 (triplet, J = 7.6 Hz, CH_2 linker) δ = 1.87 (2H, quintet, J = 7.6 Hz, CH_2 linker), δ = 1.44 (27H, doublet, J = 8 Hz).^{13}C NMR δ = 171.5 aromatic C, δ = 151.9 (C═O), δ = 141, 123.1, 122, 120, 118.2, 111 δ = 81.6 (quarternary carbon), δ = 62.8 (methoxy —OCH_3) aromatic C, δ = 55.1 piperazine ring, δ = 53.4 Cyclen ring Carbon, δ = 53.4 piperazine ring, δ = 50.6 alkyl group linker, Cyclen ring carbon δ = 28.2 alkyl carbon CH_2 carbon linker ($C(CH_3)_3$), δ = 26.1. MS (ESI +) *m/z* calculated for $C_{37}H_{64}N_6O_7$ is 704.483 found $(M + H)^+$ is 705.4908 and $(M + K)^+$ is 743.4422.

2.1.4. 2-(4,7-Bis-carbamoylmethyl-10-(3-(4-(2-methoxy-phenyl)-piperazin-1-yl)-propyl)-1,4,7,10teraaza-cyclododec-1-yl)-acetamide (4)

Compound 3 was dissolved in dichloromethane and 1 ml of trifloroacetic acid was added and reaction mixture was allowed to stir at room temperature for 24 h. Then the solvent was evaporated, and residue was re-dissolved in DCM and washed with 10% aqueous solution of NaOH to make the pH 9 of reaction mixture. Further solution was evaporated and resulting product was used as such without any purification. To a solution of resulted product (100 mg, 0.247 mmol) and K_2CO_3 (102.56 mg, 0.742 mmol) in acetonitrile, bromo-acetamide (101.84 mg, 0.247 mmol) dissolved in acetonitrile was added dropwise. The reaction mixture was refluxed at 65 °C and the reaction mixture was allowed to stir for additional 24 h. Then reaction mixture was filtered, and inorganic salts were filtered, and solution was evaporated to dryness under vacuum. The residue was dissolved in water and diethyl ether was added to remove nonpolar impurities. ^{1}H NMR was recorded in deuterated DMSO where as ^{13}C NMR in deuterated H_2O because amide hydrogens are superimposed (broad spectra obtained) in deuterated water (individual peaks are not clearly visible) and in ^{13}C NMR due to presence of residual water in deuterated DMSO peaks intensity is very low. So, ^{1}H NMR(400 MHz, DMSO) (δ in ppm) δ = 8.00 (4H, s) –NH_2 amide, δ = 7.94 (2H, s) –NH_2 amide, δ = 7.14 (4H, s, br) aromatic H, δ = 5.37 (2H, triplet, J = 5.6 Hz), δ = 3.7 (17H s, br) ((3H, OCH_3, 8H piperazine ring , 6H CH_2 adjacent to NH_2)), δ = 3.3 (DMSO residual water), δ = 2.50 (quintet 3H, DMSO), δ = 2.04 (18H, s) (16H Cyclen ring Hydrogens, 2H alkyl linker), δ = 1.18 (2H, J = 5.6 Hz, triplet). ^{13}C NMR (400 MHz, deuterated water) δ = 173.9 (Carbonyl oxygen of amide pendant arm), δ = 169.2 (aromatic carbon), δ = 134.9, 134.0, 128.7, 128.5, 128.3 (five aromatic carbons), δ = 68.1 (amide pendant arm), δ = 67.02 (methoxy carbon), δ = 51.2 (piperazine ring carbon), δ = 48.1 (Cyclen ring), δ = 30.1, 28.9, 24.5 (linker carbon). MS (ESI +) *m/z* calculated for $C_{28}H_{49}N_9O_4$ is 575.3921 and found $(M + H)^+$ is 576.3990, $(M + Na)^+$ 598.3814 and $(M + K)^+$ 614.3540.

2.1.5. Preparation of (lanthanide) Gadolinium (III) complex of DO3AM-MPP (5)

To a solution of DO3AM-MPP (50 mg, 0.0869 mmol) (4) in water was added a solution of Gadolinium nitrate (32.32 mg, 0.0869 mmol) aqueous solution. The pH of solution was maintained between 4 and 5 by addition of 1 M aqueous solution of KOH. The reaction was heated at 60 °C for 24 h and solvent was evaporated under vacuum to obtain Gadolinium-complex as pure white solid. HRMS-ESI-MS calculated for $C_{28}H_{51}GdN_9O_5^{3+}$ $((M + H_2O)/3)^{3+}$ *m/z* = 250.4413 and found $((M + H_2O)/3) + H)^{3+}$ =251.2000

2.1.6. Preparation of (lanthanide) Europium (III) complex of DO3AM-MPP (6)

To a solution of DO3AM-MPP (50 mg, 0.0869 mmol) (4) in water was added a solution of Europium Chloride (31.86 mg, 0.0869 mmol) in aqueous solution. The pH of solution was maintained between 4 and 5 by addition of 1 M aqueous solution of KOH. The reaction was heated at 60 °C for 24 h and solvent was evaporated under vacuum to obtain Europium complex as cream white solid. ^{1}H NMR (400 MHz, D_2O) (δ in ppm) δ = 7.91(–NH_2 amide, 6H), δ = 7.31–7.23 (m, aromatic hydrogens, J = 6 Hz), δ = 5.15 (quintet, piperazine ring, 8H, J = 4.4 Hz), δ = 5.0 (s, 16H, cyclen ring) δ = 4.17 (t, 2H, linker J = 6.4 Hz), δ = 3.9 (–OCH_3, methoxy group) δ = 2.52 (2H, t, J = 6.4 Hz), δ = 2.23 (quintet, 2H, J = 6.4 Hz); HRMS-ESI-MS calculated for $C_{28}H_{51}GdN_9O_5^{3+}$ $((M + H_2O)/3)^{3+}$ *m/z* = 248.7736 and found $((M + H_2O)/3) + 3H)^+$ =251.1822

2.2. CEST parameters

2.2.1. Luminescence lifetime measurement

The luminescence lifetime (τ_m) and q value measurements were recorded on HIDEX Instrument. τ_m for Eu-DO3AM was calculated by measuring the variation in luminescence count with a change in decay time. The measurements were carried in water and deuterated water (pH 7.4). The source used for analysis was a hydrogen flash lamp. Slit widths for emission and excitation were kept open. The intensity decay curves were obtained at emission maximum and fitted as the sum of exponential

$$I_t = I_o \sum A_i e^{-\frac{t}{\tau}}$$

Where τ and A represent the fluorescence lifetime and pre-exponential factor, respectively.

The number of water molecules coordinated to the inner sphere (q) of the complex is calculated from luminescence rate constants in water and heavy water using the equation given by Supkowski and Horrocks:

$$q = A_{Eu}\left(\frac{1}{\tau_{H_2O}} - \frac{1}{\tau_{D_2O}} - a_{Eu}\right)$$

Where τ_{H2O} & τ_{D2O} represent luminescence lifetime of Eu-DO3AM-MPP in H_2O and D_2O. The value of A_{Eu} = 1.1 ms^{-1} and a_{Eu} is 0.31 ms^{-1}. a_{Eu} is used for the correction of an error, which accounts for closely diffusing OH oscillators.

2.2.2. Relaxometric Studies: In vitro studies

MR Imaging was done using a 7 T Bruker Biospec USR 20/70 animal MRI scanner at AIIMS, Delhi. Rare $T_1 + T_2$ sequence was used to obtain relaxivity. In vitro and in vivo T_1 and T_2 measurements were performed at 37°C with eight different TR repetition time (8 ms, 24 ms, 40 ms, 56 ms, 72 ms, 88 ms, 104 ms, 120 ms) and TE echo time (5376 ms, 2876 ms, 1376 ms, 676 ms, 376 ms, 176 ms, 26 ms, 11.59 ms). MRI experiments to measure the change in longitudinal relaxivity (r_1) were performed with six different concentrations of Gd-DO3AM-MPP (0.625–8 mM, pH-7). Agar (1% in water) was added to all solutions for maintaining homogeneity. The relaxivity at different concentration was calculated using the equation:

$$\mathbf{r}_{1,obs} = \left(\frac{1}{\mathbf{T}_{1,obs}} - \frac{1}{\mathbf{T}_{1,d}}\right)[\mathbf{GdL}]$$

where $1/T_1$ is the relaxation rate and $1/T_1$, d is the solvent's diamagnetic contribution, and (GdL) is the concentration of complex in mM. Relaxation data were analyzed with Topspin 2.0 Bruker Software, and the relaxivity (r_1 & r_2) measured by regression analysis.

2.3. Physiochemical characterization

2.3.1. Equilibrium measurements

Potentiometric titrations were used to determine protonation con-

stant (pka) of DO3AM and stability constant (β) of the complexes with Gd^{3+}, Eu^{3+}, Cu^{2+}, and Zn^{2+} using Metrohm potentiometer. The protonation constants were measured by titrating 0.5 mM ligand with 0.01 M tetramethylammonium hydroxide (TBAOH) at 25℃ in the pH range 2–14. The protonation constant was calculated according to the equation

$$K_i = \frac{[\mathbf{H_iL}]}{[\mathbf{H_{i-1}L}][\mathbf{H^+}]}$$

where i = 1, 2, 3

Stability constants of DO3AM-MPP were determined by potentiometric titration of 1:1 Metal: Ligand solutions. Solutions of metal salts were prepared by dissolving the appropriate amount in Milli-Q water and titrated with tetra-butyl ammonium hydroxide. Stability constants of the metal complex were evaluated as per the equation:

$$\beta = \frac{[\mathbf{MH_iL}]}{[\mathbf{MH_{i-1}L}][\mathbf{H^+}]}$$

Where i = 1, 2, 3

2.3.2. Kinetic stability

Kinetic stability is an important parameter for Gadolinium complexes as these are used in MRI as contrast enhancement. The extent of dissociation of gadolinium complexes depends on the selectivity of ligands with gadolinium ion over endogenous metal ion present in body fluids. As in vivo, endogenous cations (Fe^{3+}, Ca^{2+}, Zn^{2}+, and Cu^{2+}) may react with Gadolinium chelates by displacing Gd^{3+} in a metal–metal *trans*-metalation exchange. Thus, to understand the in vivo fate of the Gd^{3+} containing contrast agent, we must know the rate of the exchange reaction of Gd–DO3M-MPP with Eu^{3+} and Zn^{2+}. The formation of Eu^{3+} and Zn^{2+} complexes at 276 and 332 nm were used to study the metal exchange rate in Gd–DO3AM-MPP. The concentration of the complex Gd-DO3AM-MPP taken was 1 mM, whereas the Europium concentration was used 10-15fold excess and that of Zinc metal ion was 30–40 times higher, respectively, confirming pseudo-first-order conditions. The temperature was kept constant at 25 °C, and the ionic strength maintained with 2 M KCl at pH 7.4. In the presence of an excess of the exchanging ion, the *trans*-metalation process may be assumed to be a pseudo-first-order process, and the rate of reaction can be expressed with the equation:

$$\mathbf{A_t} = (\mathbf{A_0} - \boldsymbol{A_p})\boldsymbol{e} - \boldsymbol{k_{obs}t}$$

where k_{obs} is a pseudo-first-order rate constant, A_t is the absorbance values at time t, A_o is the absorbance values at time t = 0, and A_p is the absorbance values at time t = equilibrium point.

2.4. Fluorescence studies

2.4.1. Fluorescent emission of Eu-DO3AM-MPP

Fluorescence emission spectra of varying concentrations of Eu-DO3AM (10 μm −100 μm) were recorded using 300 to 700 nm on Synergy 2 multi-reader (M/S Biotech Instruments, USA) with excitation at 276 nm.

2.4.2. Fluorescence quenching

The experiment was performed as reported previously. Briefly, the concentration of serotonin (=fluorophore, 0.1 μM in Phosphate Saline buffer) was fixed, and dilutions of Eu-DO3AM-MPP (10 μM-100 μM) (quencher) were prepared in Milli-Q water. In a 96 well black opaque plate, 10 μl of serotonin was incubated with different ligands concentrations. The final volume in each well was 200 μl. The solutions were mixed thoroughly and allowed to incubate for 30 min. The fluorescence emission was recorded from 300 nm to 700 nm using Synergy 2 Multi-Mode reader (M/S Biotech Instrument USA) with excitation at 260 nm. The experiments were carried out at room temperature. The background emission from phosphate buffer and Milli-Q water was subtracted from the sample emission. The data reflected a change in fluorescent emission with quencher concentration and was plotted following the Stern-Volmer Equation.

Mechanism of quenching. To establish the quenching mechanism of the ligands on serotonin, the Stern-Volmer equation was used for analysis.

$$\frac{F_O}{F} = 1 + K_{SV}[q]$$

where: F_O = Fluorescence intensity of pure Serotonin (negative control) F = Fluorescence intensity of Serotonin + analog: K_{SV} = biomolecular quenching constant: [q] = molar concentration of quencher (ligand Eu-DO3AM)

2.4.3. 5-HT_{1A} receptor binding assay through fluorescence studies

The hippocampus of the Sprague Dawley rat brain was homogenized in 10 volumes of ice-cold PBS buffer (50 mM, pH 7.4) using an Ultra Truax T10 (IKA) and centrifuged at 3000 rpm for 20 min. The resulting pellet was suspended using an Ultra Truax and centrifuged again at 3000 rpm for 20 min. A similar procedure was repeated. The obtained pellet was resuspended in 10 volumes of buffer and stored at −80℃ until used in receptor binding assays. The purity of extracted serotonin protein was confirmed by measuring absorbance ratio at 260, and 280 nm, which conforms to the protein obtained from Westar rats (1.86 mg/ml protein), is more than 95% pure. The binding of protein with synthesized ligands was studied through fluorescence quenching of the protein. The free amount of ligand which did not bind to the serotonin was calculated using the following equation:

(Free Ligand = Total Conc of ligand used – ((Q)* (Conc of serotonin))

Scatchard plot is plotted using following equation:

$$\frac{\boldsymbol{Q}}{\boldsymbol{LigandFree}} = -\frac{1}{\boldsymbol{k_d}(\boldsymbol{Q})} + \frac{\boldsymbol{n}}{\boldsymbol{k_d}}$$

Non-specific binding was performed using 100fold excess of serotonin and MPP.

2.4.4. Characterization of Gd-DO3AM-MPP using power X-ray diffraction

Powder X-ray diffraction analysis was performed using the Bruker D8 Discover instrument at the University of Delhi. The Cu-Kα radiation was used in the source, and the instrument was operated at 40 kV and 40 mA. The XRD patterns were recorded within 10-50° range of 2θ as a function of intensity with a scanning rate of 2°/min. The miller indices (*hkl*) were calculated using Bragg's Equation and XRD pattern was plotted using Origin7.

2.5. Computational modeling

The geometry of Gd-DO3AM-MPP and Gd-DO3AM-MPP-H_2O in aqueous solution (including water molecule in the inner sphere) were optimized ab initio with DFT calculations on Gaussian 09 software. [15] Hybrid functional B3LYP and MWB53 [16] basis sets for Gadolinium and 6-31G* for C, H, N, and O were chosen to compute the energy difference between two conformations. After optimization (cartesian input coordinates of Gd-DO3AM-MPP in ESI Table S1), the complexes were obtained in a square ant prismatic geometry. Energies of optimized complexes were calculated after convergence. The PDB files generated were further used for docking studies. Docking studies to visualize the interaction between the complex (Gd-DO3AM-MPP) and receptor 5-HT_{1A} were accomplished on the Glide module of Schrodinger molecular modeling software.

2.6. MTT assay

MTT assay was conducted to analyze the cytotoxicity of the Gd-DO3AM-MPP complex on HEK (Human Embryonic kidney) cell lines.

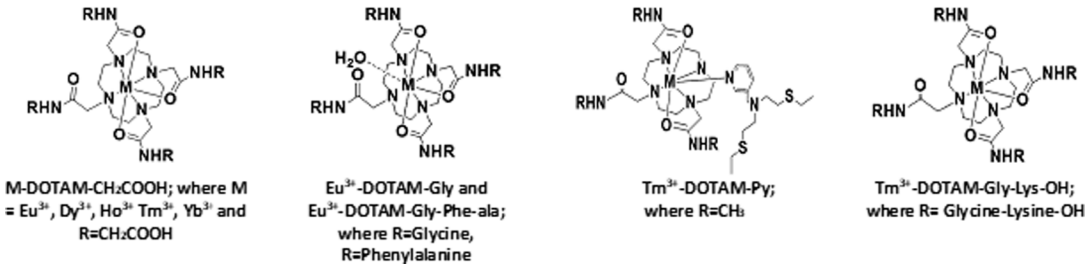

Fig. 2. PARACEST Agents with different application.

In a 96 well plate, growing cells were seed at a density of 4000 cells/wall. Cells were treated with varying concentrations of the Gd-DO3AM-MPP complex ranging from 100 mM to 1pM. At predefined intervals of 24 h, 48 h and 72 h the cells were washed and replenished with fresh media to ascertain the cytotoxicity of the Gd-DO3AM-MPP complex. Further cells were treated with MTT 3-(4,5-dimethyl-2-thiazolyl)-2,5-diphenyl-2Htetrazolium bromide (concentration 0.05 mg/ml) for two hours so that cells convert the MTT (blue colored) into Formazan crystals (purple). Addition of DMSO led to solubilization of formazan crystal and optical density of these crystals were measured at 570 nm. HBBS (Hank's Balances salt solution) were used as negative control. The experiment was performed in triplicate.

2.7. In vivo MR imaging

In vivo MR imaging was performed in All India Institute of Medical Sciences Delhi, India using Biospec USR 70/20 7 T animal MRI Instrument on two mice (male sex and age 8 weeks, breed BALB/C). One mice was considered as control which was injected with saline. The second mouse was sedated with ketamine/xylazine with a concentration of 17.5 mg/ml and 2.5 mg/ml respectively. Respiration pulse was monitored during the whole experiment and maintained at 90 beats/min. In addition, for the estimation of 5-HT_{1A} binding affinity of Gd-DO3AM-MPP in the hippocampus region of the brain, the mice was injected with 0.625 mM concentration of Gd-DO3AM-MPP intravenously (as brighter contrast obtained at 0.625 mM concentration of Gd-DO3AM-MPP), after rupturing the Blood-Brain-Barrier with 25% w/v of mannitol. MR Imaging was performed in the mice using $T_1 + T_2$ map Rare sequence with a scanning time of 54 min.

3. Results and discussion

3.1. Design consideration

Gadolinium complexed in the macrocyclic cage of DOTA (2,2′,2′′,2′′′-(1,4,7,10-teraazacyclododecane-1,4,7,10-tetraethyl) tetra-acetic acid) or DO3A (2,2′,2′′-(1,4,7,10-teraazocyclododecane-1,4,7-triyl) tri-acetic acid) has been the preferred strategy to develop paramagnetic contrast agents due to the complex's excellent kinetic inertness and thermodynamic stability, making it suitable for in vivo applications. Retaining the same scaffold of Gd-DOTA, researchers have developed paramagnetic CEST agents. The modification focuses on introducing labile protons (–NH, –OH) that can be exchanged with bulk water protons in tissues. For example, Markwood and co-workers synthesized pH-responsive gadolinium-cyclen contrast agents with carboxylate and amide side chains as CEST agents. [17] Other examples are Ln-DOTAM-Gly [18] and Yb-DOTAM [19] as a pH-responsive probe, Tm-DOTAM-βAla-py [20] for imaging of endogenous zinc and copper and Eu-DOTAM-Glu-Lys-OH and Tm-DOTAM-Glu-Lys-OH[21] to study their magnetic properties (Fig. 2).

The replacement of carboxylates with amides provides reduced electron density at the metal centre, leading to a slow exchange of

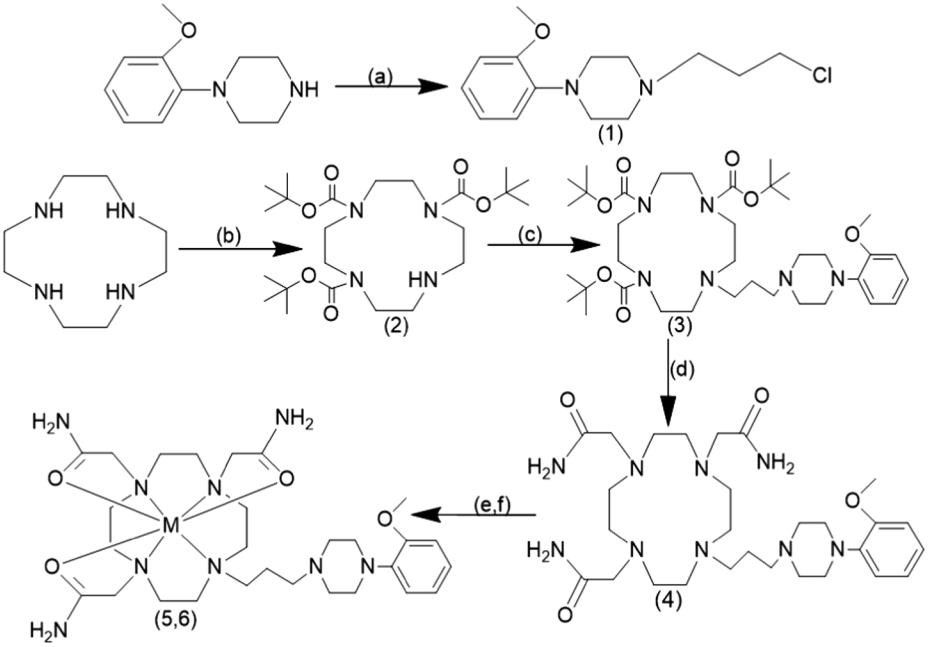

Scheme 1. Where M = Gd^{3+}, Eu^{3+}. (a) Br-CH_2-CH_2-Cl, K_2CO_3, acetonitrile, 70°C (b) $((CH_3)_3CO)_2O$, Et_3N, chloroform, 0°C, (c) K_2CO_3, acetonitrile. (d) TFA/DCM, $BrCH_2CONH_2$, acetonitrile, 70°C (e) $GdCl_3{\cdot}6H_2O$, water, 0.1 M NaOH 70°C (f) $EuCl_3{\cdot}6H_2O$, water, 0.1 M NaOH, 70°C.

exchangeable protons at the metal centre to the tune of 1–3 ms [22,23]. This variation resulted in compromised thermodynamic stability. However, it was reasonably compensated by the high kinetic inertness [24].

As the fourth arm of DOTA remains free, targeting was achieved by appending the serotonin 5-HT_{1A} receptor known antagonist pharmacophore, MPP. Scheme 1 includes the synthesis and structure of the Para-CEST agent.

The first step involved MPP functionalization through 1-bromo, 3-chloro propane linker (1) synthesized in more than 75% yield. The formation of the compound was asserted by the appearance of two triplets and quintet in ^{1}H NMR. Compound (1) was appended with triprotectedboc-cyclen (2). After TFA/DCM deprotection, the compound (3) was alkylated with bromo-acetamide with an overall yield of 60 ± 5% for the purified product. Loading of Gadolinium and Europium was accomplished by complexing metal chloride (metal = Gadolinium or Europium) with ligand DO3AM-MPP. Mass spectrometry confirmed the formation of Gd-DO3AM-MPP and Eu-DO3AM-MPP (Isotopic Pattern) (ESI-MS).

3.2. CEST parameters

The parameters governing CEST contrast are similar to those governing T_1 contrast and includes (i) water residence lifetime (τ_m) (ii) no of water molecules coordinated to the inner sphere (q) (iii) T_1 and T_2 relaxivity of surrounding water protons and (iv) $r_{Gd\text{-}H}$ distance between Gadolinium and a coordinated water molecule. [25]

3.2.1. Luminescence based evaluation of (i) water residence time and (ii) number of water molecules

The exchange rate of water protons with bulk water protons of tissues depends on the metal ion apart from other physical parameters viz., pH, temperature, and ionic environment. Ideally, for a CEST agent, the metal-bound water residence lifetime (τ_m) should range from 10^{-5} to 10^{-2} s. In the case of cyclen derived contrast agents, the change in the rate can be introduced by variation of side pendant arms design. The replacement of acetate in DOTA/DO3A with the amide in DO3AM results in the slow exchange of metal-bound water molecules, presumably because the pendant arms of DOTA or DO3A contain acetate groups, which more basic as compared to DO3AM amide arms. Thus, the metal center interacts strongly with DO3A/DOTA in comparison to the water molecule. On the other hand, in DO3AM, the metal center interacts strongly with water molecules leading to higher residence time/ slower exchange.

The nature of the metal ion also influences the water exchange rate. Gadolinium-DOTA complexes have a faster exchange rate than the Europium-DOTA complexes, which are of the order of »100-300 ns. [26]

The number of water molecules (q) in the first coordination sphere of the metal complex for optimization also determines the complex's relaxivity and stability.

Luminescence lifetime measurements of water molecules bonded to the metal ion can provide information about the hydration state. In contrast to Gadolinium, Europium and terbium are most studied lanthanide ions due to their longer excited-state lifetime. Europium and Gadolinium are the neighboring elements in the periodic table and share many fundamental properties like ionic radius, chemical reactivity, and valency. However, Europium possesses one extra physical property luminescence under UV light, which is not shown by Gadolinium. Due to resemblance in fundamental properties, Europium analog Eu-DO3AM-MPP can be used in place of Gadolinium Gd-DO3AM-MPP to monitor the physical processes Luminescence and tissue distribution through fluorescence. Among all the lanthanides, Europium has found to have a slower rate of water exchange and low paramagnetic relaxation enhancement. (maximum T_1 and T_2 shortening effect). These properties of Europium are favorable in the design of the PARCEST agent. [27] The decay of excited Eu^{3+}-DO3AM-MPP complex was measured in H_2O and D_2O as a concentration function. As well documented, the O-H — oscillator (in H_2O) is an effective quencher for the excited lanthanide ion compared to the O-D oscillator of D_2O.

Thus, there is a difference in quenching frequencies of O—H and O-D bonds that can estimate the number of coordinated water molecules. The luminescence lifetime of Eu-DO3AM (pH 7.4 and $7F_0$ to $5D_0$ transition) was found to be 0.23 ms in H_2O and 0.38 ms in D_2O at 25 °C. Using the Supkowski and Horrocks equation. [28] The hydration number of Eu-DO3AM was calculated to be 1.43, which confirms mono aqua complex formation.

3.2.2. MRI based evaluation of (iii) NMR relaxivity: In vitro studies

The longitudinal (T_1) and transverse (T_2) relaxation time of Gd-DO3AM-MPP were measured as a function of concentration to determine the longitudinal relaxivity (r_1: $r_1 = 1/T_1$) and transverse relaxivity (r_2: $r_2 = 1/T_2$). Linear enhancement was obtained for $1/T_1$ and $1/T_2$ with the [Gd-DO3AM] (r = 0.999 for $1/T_1$ and r = 0.985 for $1/T_2$), as depicted in Fig. 3(b) & (c) respectively. The longitudinal relaxivity r_1 and transverse relaxivity r_2 were 5.85 $mM^{-1}s^{-1}$ and 6.41 $mM^{-1}s^{-1}$, respectively, on 7 T at 37 °C (see Fig. 3).

The Gadolinium loaded complex showed shortening in relaxation time with respect to water ($T_{1\ pure\text{-}water}$ = 2916.79 ms and T_1 = 305.703 ms and $T_{2\ pure\text{-}water}$ = 112.643 ms and T_2 = 42.241 ms at a lower concentration. . At [Gd-DO3AM-MPP] = 0.625 mM, an increase in enhancement and brightest contrast was recorded; however, increasing [Gd-DO3AM-MPP] lead to the formation of a darker image. The linear enhancement with an increase in the ligand concentration, followed by darker contrast at [Gd-DO3AM-MPP] = 8 mM, can be attributed to the saturation achieved between the energy levels. [30] (see Fig. 3).

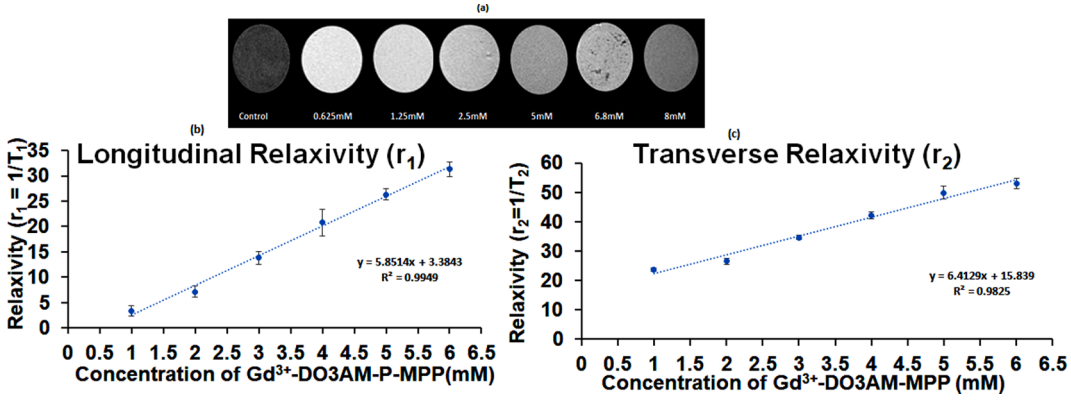

Fig. 3. (a) T_1 Weighed MRI Contrast Images of Gd^{3+}-DO3AM-MPP at a different concentration ranging from 0.625 mM to 8 mM, and 3(b) show the linear regression analysis of relaxivity of Gd^{3+}-DO3AM-MPP complex with concentration to determine longitudinal relaxivity (r_1) and 3(c) transverse relaxivity (r_2) respectively.

Table 1
pka values of ligands.

pka	DOTA[33]	DO3A-MPP	DO3AM-MPP
pka1	11.14 ± 0.02	9.93 ± 0.02	9.12 ± 0.02
pka2	9.69 ± 0.01	6.72 ± 0.06	6.09 ± 0.03
pka3	4.85 ± 0.07	4.65 ± 0.01	4.02 ± 0.02

Table 2
Stability Constant of metal complexes.

Stability Constant	DOTA[34]]	DO3A-Propyl-MPP	DO3AM-Propyl-MPP
$Log\beta_{GdL}$	23.2 ± 0.01	17.6963 ± 0.03	13.7439 ± 0.04
$Log\beta_{EuL}$	24.5 ± 0.06	17.3245 ± 0.02	13.5486 + 0.06
$Log\beta Zn_2L$	18.1 ± 0.06	7.1879 ± 0.05	11.3860 ± 0.08
$Log\beta Cu_2L$	22.2 ± 0.03	6.0102 ± 0.03	18.0548 ± 0.01

Table 3
Pseudo First order rate constants characterizing the metal exchange reactions of Gd^{3+}-DO3AM-MPP with Eu^{3+} and Zn^{2+}.

Metal-Ligand Complex	Eu^{3+}	Zn^{2+}
Gd-DOTA[36]	2.1×10^{-5}	Not observed
Gd-DO3A[37]	2.3×10^{-3}	1.4×10^{-2}
Gd-DO3AM-MPP	3.5×10^{-6}	3.4×10^{-5}

3.3. Physicochemical characterization

3.3.1. Equillibrium Measurements

The complexation properties of DO3AM-MPP are different from DOTA and DO3A due to three amide groups. The differences in the stability constants of complexes formed between DO3AM and metal ions were determined using potentiometric titration. The metal selected were lanthanide trivalent ions (Eu^{3+}) and biologically significant divalent metals ions (Zn^{2+}, Cu^{2+}). The pKa's are summarized in Table 1 .

It was observed that the pka values of DO3AM are lower than corresponding DOTA and DO3A due to the difference in amide and acetate arms basicity. Similarly, stability constant (Logβ, Table 2) of DO3AM complexes are lower than DOTA due to weaker Ln^{3+}-amide oxygen bond in DO3AM than Ln^{3+}-acetate oxygen bond in DOTA or DO3EA. [35] The stability constant of Gd-DO3AM-MPP is slightly higher than Eu-DO3AM-MPP due to lanthanide contraction, which leads to an increase in electron density on the metal and consequently, a weak coordinate bond between amide oxygen and metal ion.

3.3.2. Kinetic stability

To avoid the toxic effects of free Gadolinium, trans-metalation of Gadolinium with endogenous metal cation should not occur. The extent of dissociation of Gd-DO3AM-MPP was estimated from the kinetics of exchange reactions. The exchange rate constant of Gd-DO3AM-MPP was investigated in the presence of Eu^{3+}, and Zn^{2+} metal ion and value of proton assisted exchange rate constants are summarised in Table 3.

(Gd^{3+}-DO3AM-Propyl-MPP) + M^{n+} (M^{n+}-DO3AM-Propyl-MPP) + $Gd^{3+}$where M^{n+} =Cu^{2+}, Eu^{3+})

The exchange rate of Gd-DO3AM-MPP with Eu-DO3AM-MPP and Zn-DO3AM-MPP is very low compared to DO3A or DOTA derivatives due to lower basicity of amide oxygen atom which conforms higher kinetic inertness to Gd-DO3AM-MPP over Gd-DOTA, making it suitable for in vivo application. The plausible explanation lies in already existing mechanistic data. [38] According to which acid-catalyzed dissociation of the Ln-DO3AM complex occurs by a different mechanism as compared to Ln-DOTA. In Ln-DOTA, the first step is the protonation of the uncoordinated carboxylate oxygen atoms followed by the proton transfer to ring nitrogen. The electrostatic repulsion between now positively charged nitrogen and Ln (III) metal ion facilitates the expulsion of Ln (III) metal ion from the cage. In Ln-DO3AM, due to weaker electrostatic interaction between Ln^{3+} ion and the neutral ligand DO3AM, it is much challenging to protonate neutral arm as compared to negatively charged acetate arm which ultimately results in limiting their rate of acid-catalyzed dissociation. Although stability constant values of Gd-DO3AM is much less than Gd-DOTA or Gd-DO3A, high comparable kinetic inertness of Gd-DO3AM with Gd-DOTA makes it suitable for CEST Imaging.

3.3.3. $r_{Gd\text{-}H}$ distance between gadolinium and coordinated water

The distance between the water molecule and Gadolinium was evaluated theoretically using the Gaussian software Fig. 4. The unsolvated Gd-DO3AM-MPP was found to have lower energy than the solvated Gd-DO3AM-MPP with a difference in energy (DE = E[*Gd-DO3AM-MPP*]-$_{Solv}$ -E[*Gd-DO3AM-MPP*]-$_{Unsolv}$) of 7.31 kJ/mol. The unstabilization of solvated Gd-DO3AM-MPP is due to the presence of a water molecule in the inner coordination that weakens the coordination bonds of Gd^{3+} with other pendant arms. The distance of the coordinated water molecule from Gd^{3+} is 2.7 Å, which is in fair agreement for the NMR relaxometry experiment. [32]

3.4. Targeting capability

3.4.1. & 3.4.2 Binding constant through fluorescence quenching studies

Fluorescence provides information about the molecular environment in the vicinity of the chromophore molecule. Fluorescence quenching studies were performed to evaluate the binding constant between the ligand (quencher:(Eu-DO3AM-MPP)) and protein (5-HT_{1A} receptor). The incremental addition of Eu-DO3AM-MPP (UV plot of Eu-DO3AM-MPP λ_{max} 276 nm, ESI Figure 16) resulted in the reduction of fluorescence intensity for 5-HT_{1A}) Fig. 5. Under the experimental conditions, Eu-DO3AM-MPP illustrated no fluorescence emission in the range 300–400 nm and did not affect serotonin intrinsic fluorescence. As

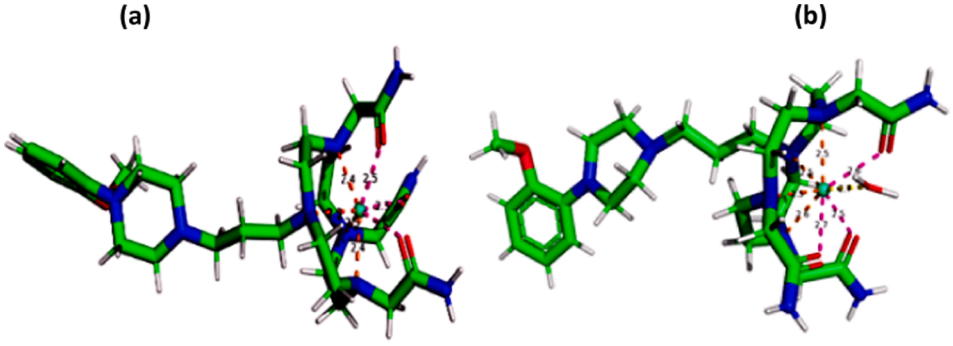

Fig. 4. DFT minimized the structure of (a) Unsolvated Gd-DO3AM-MPP (b) solvated Gd-DO3AM-MPP. The presence of water molecules in the inner coordination sphere destabilizes the coordination bonds reflected in increases in distances, thereby giving an energy difference of E [Gd-DO3AM-MPP]-$_{Solv}$ -E[*Gd-DO3AM-MPP*]-$_{Unslov}$ of 7.31 kJ/mol. The $r_{Gd\text{-}H}$ is 2.7 Å.

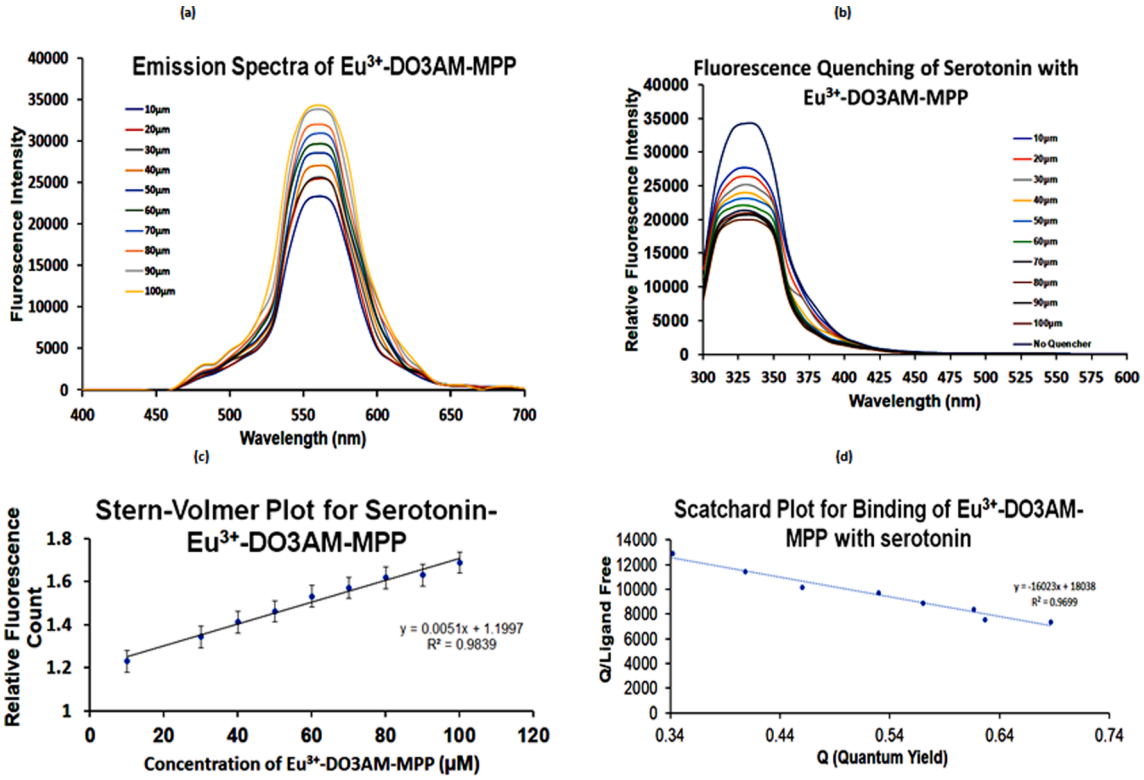

Fig. 5. (a) Emission Spectra of Eu-DO3AM-MPP with Excitation at wavelength 276 nm (b) Fluorescence spectra of serotonin ($\lambda_{emission}$ 330 nm) with varying concentration of Eu-DO3AM-MPP (c) Stern-Volmer Plot of Serotonin-Eu-DO3AM at 25°C (d) Scatchard plot for Serotonin-Eu-DO3AM-MPP at 25°C.

deduced by the Stern Volmer plot and equation [39]) (Fig. 5c), the association constant, K_{SV} was found to be 0.0051 (micro M)$^{-1}$.

3.4.3. Binding affinity assay

The specific binding of Eu-DO3AM-Propyl-MPP with 5-HT_{1A} receptor was estimated through the saturation binding assay. 5-HT_{1A} receptors isolated in murine brain hippocampal homogenate were incubated with the complex. [40] Specific binding was calculated by Scatchard plot analysis (Fig. 5d), which revealed the high affinity of Eu-DO3AM-MPP towards neuronal hippocampus receptor with k_d value 62 ± 0.02 pM. Non-specific binding was calculated by using a 100 fold excess of serotonin and methoxyphenyl piperazine.

3.4.4. Characterization of Gd-DO3AM-MPP using power X-ray diffraction

The obtained powder XRD pattern for Gd-DO3AM-MPP resembles well with monoclinic symmetry with space group P12/c1 (ICSD Number 98–010-9886), which confirm the presence of Gadolinium and other chemical constituents and, therefore, supports the chelating affinity of the synthesized complex. The crystal parameters and pattern for the Gd-DO3AM-MPP are depicted in Table S1 and Fig. 7, respectively. It was analysed that due to the presence of organic moiety in Gd-DO3AM-MPP XRD pattern is amorphous.

3.5. Theoretical docking studies

Theoretical docking studies gave an insight into the interactions between ligand Gd-DO3AM- MPP and 5-HT_{1A} receptors. The ligand

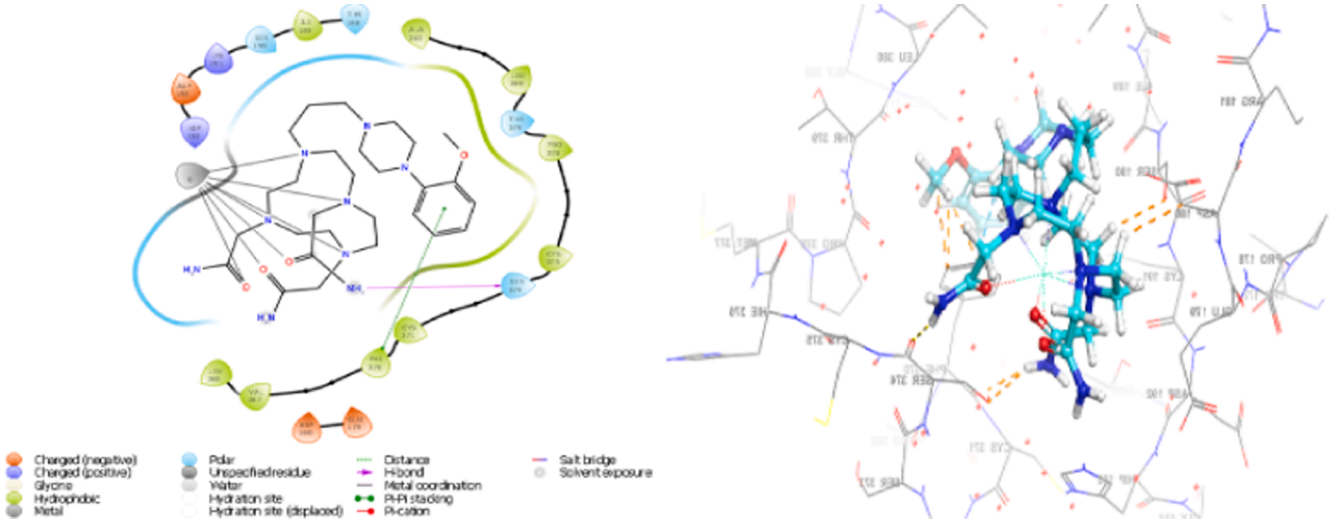

Fig. 6. (a) and (b) 3D and 2D Ligand Interaction Diagram of Gd-DO3AM-MPP with 5-HT_{1A} receptor.

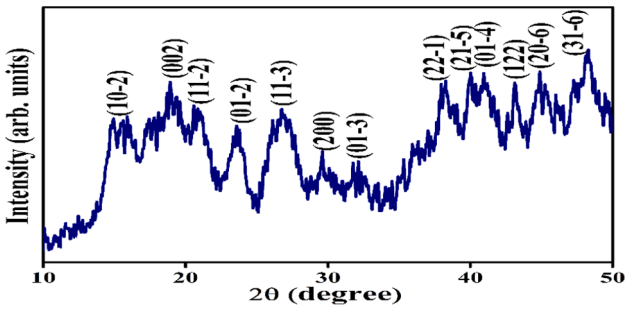

Fig. 7. Powder X-ray Diffraction Pattern for Gd-DO3AM-MPP.

Gd^{3+}-DO3AM-MPP was found to dock on a 5-HT_{1A} model with a G-Score of −4.81 and binding energy −57.29 kcal/mol. Way-100635, the well-known non-metal antagonist-ligand for the 5-HT_{1A} receptor had a docking score was −7.7 (2D and 3D Ligand Interaction Diagram in ESI) under similar docking set up. The lowering of G-score may be attributed to the presence of metal and steric hindrance in Gd-DO3AM-MPP. In 2D and 3D ligand interaction diagram (Fig. 6 and Table 4), it was observed that residues Ser 182, Thr 188, Ser 190, and Ser 374 constituted the polar groups of ligand-binding pocket. One of the amide arms in DO3AM interacted through H-bonding with Arg 181. Another amide arm showed polar and covalent interaction with Lys 191 and Ser 190. The MPP piperazine was involved in polar covalent interaction with Asp116 and retained its antagonist mode of binding with the receptor.

Table 4
GScore and Ligand Interaction of DO3AM-MPP and DFT optimized Gd-DO3AM-MPP and antagonist WAY-1OO635 with 5-HT_{1A} receptor system.

Residual Interactions			
Ligand	Non-Polar Residues	Polar Residues	GScore (Kcal/mol)
Gd-DO3AM-MPP	Leu 366, Val 367, Phe370, Cys 371, Cys 375, Pro 378, Leu 380, Ala 383, Ile 189	Hip 193, Asp 192, Lys 191, Ser 190, Thr 188, Thr 379, Ser 374, Asp 180, Glu 179	−4.81
WAY-100635	Ile 189, Cys 187, Leu 380, Ile 384, Trp 387, Leu 388, Tyr 96, Phe 370, Val 367, Phe 112, Val 364, Ile 363, Val 117, Cys 120	Lys 191, Thr 188, Thr 379, Thr 200, Asp 116	−7.7

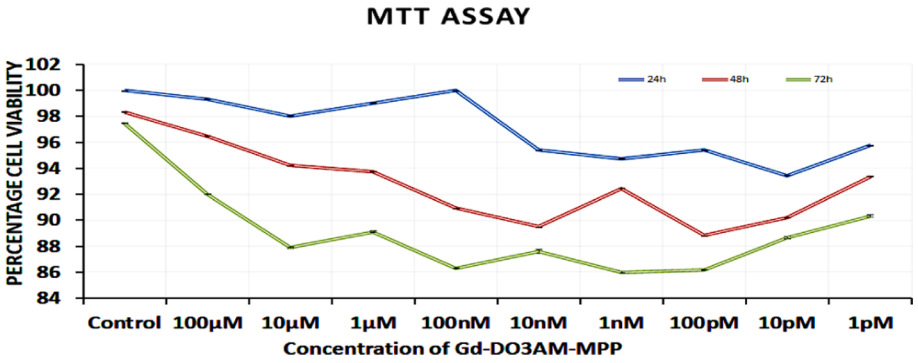

Fig. 8. MTT assay to analyse the cytotoxicity of Gd-DO3AM-MPP complex on HEK cell line.

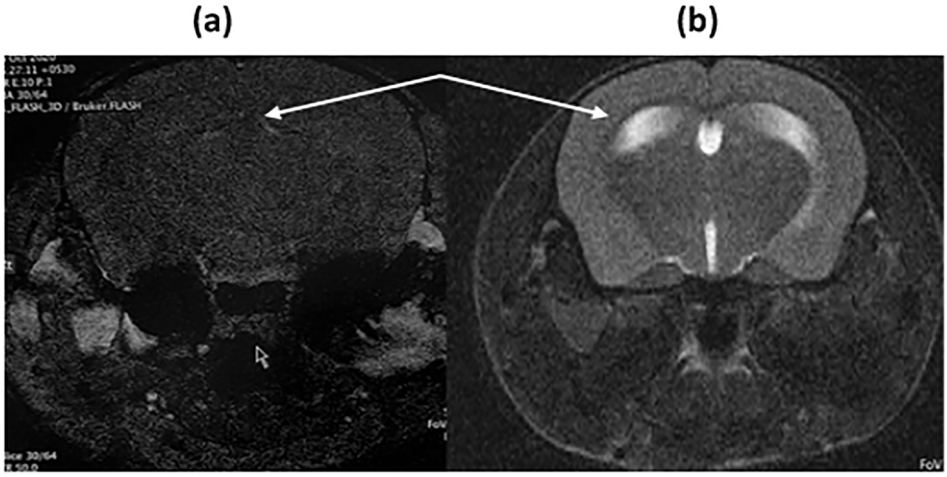

Fig. 9. In vivo MR Imaging (a) Control mice (b) showing preferential binding of Gd-DO3AM-MPP in 5-HT_{1A} receptor post injection of Gd-DO3AM-MPP contrast agent after BBB disruption with mannitol.

3.6. Cytotoxicity studies

Cytotoxicity assay was performed on HEK cell line to analyse the biological assessment of the resulting complex Gd-DO3AM-MPP using MTT as a biomarker. The toxicity of Gd-DO3AM-MPP was evaluated in the concentration range from 100 μM to 1 pM. In between concentration range 100 μm to 1 pM, maximum cells death of 9.6% was noticed after completion of 72 h (Fig. 8) which indicates the good percentage cell viability even after the prolonged time treatment. These results suggest that the Gd-DO3AM-MPP complex has minimum cytotoxicity, making it suitable for in vivo medical imaging applications.

3.7. In vivo CEST MR imaging

The longitudinal and relaxation time and binding of metal complex Gd-DO3AM-MPP in mouse was analyzed using MR Imaging technique. The Gd-DO3AM-MPP complex shows preferential uptake in the hippocampus region of the brain Fig. 9 which confirms the applicability of the complex for medical imaging purpose.

4. Conclusions

We aimed to develop a CEST-MRI contrast agent for targeting the 5-HT_{1A} receptor. The evaluation of various physicochemical parameters of DOP3AM-MPP suggests its suitability as a CEST MRI imaging agent for the mapping of 5-HT_{1A} receptors. The preclinical evaluation carried out supports the applicability of the complex in 5-HT_{1A} receptor region.

Ethical approval

All animal experiments were performed following the guidelines of the CPCSEA, Government of India, New Delhi. Animal handling and experimentation were approved by the Institutional Animal Ethics Committee (IAEC) of INMAS (Reg. No. 8/G0/RBi/S/99/CPCSEA;09-03-2014).

Declaration of Competing Interest

The authors declare that they have no known competing financial interests or personal relationships that could have appeared to influence the work reported in this paper.

Acknowledgements

DRDO, Ministry of Defense and Department of Science and Technology (DST) jointly supported this research under the project. The work was carried at the Institute of Nuclear Medicine and Allied Sciences (INMAS)-Delhi, All India Institute of Medical Sciences-Delhi, and the Supercomputing Facility for Bioinformatics and Computational Biology (SCF-BIO)-IIT Delhi. The authors gratefully acknowledge the Institutes for providing facilities and support. The authors also thank the Chemistry Department, University of Delhi, Delhi, for extending the instrumentation facilities. The authors also thank the University Grant Commission, India, for providing fellowship.

Appendix A. Supplementary material

Supplementary data to this article can be found online at https://doi.org/10.1016/j.bioorg.2020.104487.

References

[1] É. Tóth, C.S. Bonnet, Responsive ParaCEST Contrast Agents, Inorganics 7 (5) (2019) 68, https://doi.org/10.3390/inorganics7050068.

[2] A.C. Sedgwick, J.T. Brewster, P. Harvey, D.A. Iovan, G. Smith, X.-P. He, H.e. Tian, J.L. Sessler, T.D. James, Metal-based imaging agents: progress towards interrogating neurodegenerative disease, Chem. Soc. Rev. 49 (10) (2020) 2886–2915, https://doi.org/10.1039/C8CS00986D.

[3] T. Kanda, M. Matsuda, H. Oba, K. Toyoda, S. Furui, Gadolinium Deposition after Contrast-enhanced MR Imaging, Radiology 277 (3) (2015) 924–925, https://doi.org/10.1148/radiol.2015150697.

[4] L.M. De León-Rodríguez, A.F. Martins, M.C. Pinho, N.M. Rofsky, A.D. Sherry, Basic MR relaxation mechanisms and contrast agent design: MR Relaxation Mechanisms and Contrast Agents, J. Magn. Reson. Imaging 42 (3) (2015) 545–565, https://doi.org/10.1002/jmri.24787.

[5] S. Chaturvedi, A. Kaul, P.P. Hazari, A.K. Mishra, Mapping neuroreceptors with metal-labeled radiopharmaceuticals, Med. Chem. Commun. 8 (5) (2017) 855–870, https://doi.org/10.1039/C6MD00610H.

[6] G.R. Naumiec, G. Lincourt, J.P. Clever, M.A. McGregor, A. Kovoor, B. DeBoef, Synthesis of a β-CCT-lanthanide conjugate for binding the dopamine transporter, Org. Biomol. Chem. 13 (9) (2015) 2537–2540, https://doi.org/10.1039/C4OB02165G.

[7] I. Zigelboim, A. Weissberg, Y. Cohen, Target-Specific Ligands and Gadolinium-Based Complexes for Imaging of Dopamine Receptors: Synthesis, Binding Affinity, and Relaxivity, J. Org. Chem. 78 (14) (2013) 7001–7012, https://doi.org/10.1021/jo400646k.

[8] R. Varshney, S.K. Sethi, S. Rangaswamy, A.K. Tiwari, M.D. Milton, S. Kumaran, A. K. Mishra, Design, synthesis and relaxation studies of triazole linked gadolinium (III)-DO3A-BT-bistriazaspirodecanone as a potential MRI contrast agent, New J. Chem. 40 (2016) 5846–5854, https://doi.org/10.1039/c5nj03220b.

[9] N. Saini, R. Varshney, A.K. Tiwari, A. Kaul, M. Allard, M.P.S. Ishar, A.K. Mishra, Synthesis, conjugation and relaxation studies of gadolinium(iii)-4-benzothiazol-2-yl-phenylamine as a potential brain specific MR contrast agent, Dalton Trans. 42 (14) (2013) 4994, https://doi.org/10.1039/c2dt32391e.

[10] I. Zigelboim, D. Offen, E. Melamed, H. Panet, M. Rehavi, Y. Cohen, Synthesis, binding affinity, and relaxivity of target-specific MRI contrast agents, J. Incl. Phenom. Macrocycl. Chem. 59 (3-4) (2007) 323–329, https://doi.org/10.1007/s10847-007-9331-2.

[11] J. Wahsner, E.M. Gale, A. Rodr, P. Caravan, Chemistry of MRI Contrast Agents: Current Challenges and New Frontiers, (2019). https://doi.org/10.1021/acs.chemrev.8b00363.

[12] P. Caravan, C.T. Farrar, L. Frullano, R. Uppal, Influence of molecular parameters and increasing magnetic field strength on relaxivity of gadolinium- and manganese-based T1 contrast agents, Contrast Media Mol. Imaging. 4 (2009) 89–100, https://doi.org/10.1002/cmmi.267.

[13] D. Press, Synthesis , docking , and preliminary in vitro / in vivo evaluation of MPP-dithiocarbamate-capped silver nanoparticle as dual-imaging agent for 5HT 1A, 8 (2018) 19–23.

[14] P.P. Hazari, S. Prakash, V.K. Meena, N. Singh, K. Chuttani, N. Chadha, P. Singh, S. Kukreti, A.K. Mishra, Synthesis, preclinical evaluation and molecular modelling of macrocyclic appended 1-(2-methoxyphenyl)piperazine for 5-HT1A neuroreceptor imaging, RSC Adv. 6 (2016) 7288–7301, https://doi.org/10.1039/c5ra13432c.

[15] M. Frisch, G. Trucks, H. Schlegel, G. Scuseria, M. Robb, J. Cheeseman, G. Scalmani, V. Barone, B. Mennucci, G. Petersson, H. Nakatsuji, M. Caricato, X. Li, H. Hratchian, A. Izmaylov, J. Bloino, G. Zheng, J. Sonnenberg, M. Hada, D. Fox, Gaussian 09 (Revision A02), Gaussian Inc., Wallingford CT, 2009.

[16] B. Zhang, L. Cheng, B. Duan, W. Tang, Y. Yuan, Y. Ding, A. Hu, Gadolinium complexes of diethylenetriamine- N - oxide pentaacetic acid-bisamide : a new class of highly stable MRI contrast agents with a hydration, Dalt. Trans. 48 (2019) 1693–1699, https://doi.org/10.1039/c8dt04478c.

[17] M. Woods, G.E. Kiefer, S. Bott, A. Castillo-Muzquiz, C. Eshelbrenner, L. Michaudet, K. McMillan, S.D.K. Mudigunda, D. Ogrin, G. Tircsó, S. Zhang, P. Zhao, A.D. Sherry, Synthesis, relaxometric and photophysical properties of a new pH-responsive MRI contrast agent: The effect of other ligating groups on dissociation of a p-nitrophenolic pendant arm, J. Am. Chem. Soc. 126 (2004) 9248–9256, https://doi.org/10.1021/ja048299z.

[18] S. Aime, A. Barge, D.D. Castelli, F. Fedeli, A. Mortillaro, F.U. Nielsen, E. Terreno, Paramagnetic Lanthanide (III) Complexes as pH-Sensitive Chemical Exchange Saturation Transfer (CEST), Contrast Agents for MRI Applications 648 (2002) 639–648, https://doi.org/10.1002/mrm.10106.

[19] A.X. Li, F. Wojciechowski, M. Suchy, C.K. Jones, R.H.E. Hudson, R.S. Menon, R. Bartha, A sensitive PARACEST contrast agent for temperature MRI: Eu 3+-DOTAM-glycine (Gly)-phenylalanine (Phe), Magn. Reson. Med. 59 (2008) 374–381, https://doi.org/10.1002/mrm.21482.

[20] K. Srivastava, G. Ferrauto, S.M. Harris, D.L. Longo, M. Botta, S. Aime, V.C. Pierre, Complete on/off responsive ParaCEST MRI contrast agents for copper and zinc, Dalt. Trans. 47 (2018) 11346–11357, https://doi.org/10.1039/c8dt01172a.

[21] M. Suchý, A.X. Li, R. Bartha, R.H.E. Hudson, Analogs of Eu3+ DOTAM-Gly-Phe-OH and Tm3+ DOTAM-Gly-Lys-OH: Synthesis and magnetic properties of potential PARACEST MRI contrast agents, Bioorganic Med. Chem. 16 (2008) 6156–6166, https://doi.org/10.1016/j.bmc.2008.04.038.

[22] A.D. Sherry, Y. Wu, The importance of water exchange rates in the design of responsive agents for MRI, Curr. Opin. Chem. Biol. 17 (2013) 167–174, https://doi.org/10.1016/j.cbpa.2012.12.012.

[23] F. Wojciechowski, M. Suchy, A.X. Li, H.A. Azab, R. Bartha, R.H.E. Hudson, A Robust and Convergent Synthesis of Dipeptide - DOTAM Conjugates as Chelators for Lanthanide Ions: New PARACEST MRI Agents, (2007) 1625–1636.

[24] E. Terreno, Z. Baranyai, Kinetics of the Formation of [Ln (DOTAM)] 3 + Complexes, (2007) 3639–3645. https://doi.org/10.1002/ejic.200700178.
[25] L. Leone, G. Ferrauto, M. Cossi, M. Botta, L. Tei, Optimizing the relaxivity of MRI probes at high magnetic field strengths with binuclear GdIII Complexes, Front. Chem. 6 (2018) 1–12, https://doi.org/10.3389/fchem.2018.00158.
[26] S.J. Ratnakar, M. Woods, A.J.M. Lubag, Z. Kovács, A.D. Sherry, Modulation of water exchange in europium(III) DOTA-tetraamide complexes via electronic substituent effects, J. Am. Chem. Soc. 130 (2008) 6–7, https://doi.org/10.1021/ja076325y.
[27] S. Viswanathan, Z. Kovacs, K.N. Green, S.J. Ratnakar, A.D. Sherry, Alternatives to Gadolinium-Based Metal Chelates for Magnetic Resonance, Chem. Rev. 110 (2010) 2960–3018.
[28] R.M. Supkowski, W.D.W. Horrocks, On the determination of the number of water molecules, q, coordinated to europium(III) ions in solution from luminescence decay lifetimes, Inorganica Chim. Acta. 340 (2002) 44–48, https://doi.org/10.1016/S0020-1693(02)01022-8.
[30] G.E. Hagberg, K. Schef, Effect of r 1 and r 2 relaxivity of gadolinium-based contrast agents on the T 1 -weighted MR signal at increasing magnetic fi eld strengths, Contrast Media Mol. Imaging. 8 (2013) 456–465, https://doi.org/10.1002/cmmi.1565.
[32] P. Caravan, Strategies for increasing the sensitivity of gadolinium based MRI contrast agents, Chem. Soc. Rev. 35 (2006) 512–523, https://doi.org/10.1039/b510982p.
[33] M. Pniok, V. Kubíček, J. Havlíčková, J. Kotek, A. Sabatie-Gogová, J. Plutnar, S. Huclier-Markai, P. Hermann, Thermodynamic and kinetic study of scandium(III) complexes of DTPA and DOTA: A step toward scandium radiopharmaceuticals, Chem. - A Eur. J. 20 (2014) 7944–7955, https://doi.org/10.1002/chem.201402041.
[34] M. Port, J.-M. Idée, C. Medina, C. Robic, M. Sabatou, C. Corot, Efficiency, thermodynamic and kinetic stability of marketed gadolinium chelates and their possible clinical consequences: a critical review, BioMetals. 21 (2008) 469–490, https://doi.org/10.1007/s10534-008-9135-x.
[35] A. Pasha, G. Tircsó, E.T. Benyó, E. Brücher, A.D. Sherry, Synthesis and characterization of DOTA-(amide)4 derivatives: Equilibrium and kinetic behavior of their lanthanide(III) complexes, Eur. J. Inorg. Chem. (2007) 4340–4349, https://doi.org/10.1002/ejic.200700354.
[36] E. Tdth, E. Briicber, I. Lhzhr, I. Tdth, Kinetics of Formation and Dissociation of Lanthanide (III) -DOTA Complexes, (1994) 4070–4076.
[37] A. Chang, M.F. Tweedle, G.J.C. Soc, Equilibrium and Kinetic Studies of Lanthanide Complexes of Macrocyclic Polyamino Carboxylates, Inorg. Chem. 32 (1993) 587–593.
[38] G. Tircsó, E. Tircsóné Benyó, Z. Garda, J. Singh, R. Trokowski, E. Brücher, A. D. Sherry, É. Tóth, Z. Kovács, Comparison of the equilibrium, kinetic and water exchange properties of some metal ion-DOTA and DOTA-bis(amide) complexes, J. Inorg. Biochem. 206 (2020), 111042, https://doi.org/10.1016/j.jinorgbio.2020.111042.
[39] S. Aggarwal, A.K. Tiwari, P. Srivastava, N. Chadha, V. Kumar, G. Singh, A. K. Mishra, Investigation for the Interaction of Tyramine-Based Anthraquinone Analogue with Human Serum Albumin by Optical Spectroscopic Technique, Chem. Biol. Drug Des. 81 (2013) 343–348, https://doi.org/10.1111/cbdd.12073.
[40] A. Elalaoui, G. Divita, G. Maury, J.-L Imbach, R.S. Goody, Intrinsic tryptophan fluorescence of bovine liver adenosine kinase, characterization of ligand binding sites and conformational changes, Eur. J. Biochem. 221 (1994) 839–846. https://doi.org/10.1111/j.1432-1033.1994.tb18798.x.